Quantitative prediction of critical heat flux initiation in pool and flow boiling

Ding, W.; Krepper, E.; Hampel, U.;

Originally published:

November 2017

International Journal of Thermal Sciences 125(2018), 121-131

DOI: https://doi.org/10.1016/j.ijthermalsci.2017.11.022

Perma-Link to Publication Repository of HZDR:

https://www.hzdr.de/publications/Publ-26411

Quantitative prediction of critical heat flux initiation in pool and flow boiling

Wei Ding[1]*, Eckhard Krepper[2], Uwe Hampel[1,2]
[1] AREVA Endowed Chair of Imaging Techniques in Energy and Process Engineering, Technische Universität Dresden, Germany
[2] Institute of Fluid Dynamics, Helmholtz-Zentrum Dresden-Rossendorf, Dresden, Germany

Abstract

Boiling is a very efficient heat transfer mechanism with a large heat transfer coefficient and it is widely found in industrial systems. However, boiling heat transfer is limited by the critical heat flux (CHF), also termed as boiling crisis. It leads to a rapid decrease of the heat transfer coefficient in temperature controlled heat transfer or to a significant jump in heater surface temperature in power controlled heat transfer cases. While the earlier effect clearly lowers efficiency the latter may even jeopardize safety. A clear understanding of the basic mechanisms leading to CHF is still lacking. In this paper a new model of priori critical heat flux(CHF-) is derived from the bubble dynamics of nucleate boiling. It holds for pool boiling and forced convective boiling and incorporates a mutual effect model and a shear stress model. The comparison between predicted and experimental results under different thermal hydraulic conditions shows a good agreement. The model is capable to explain the initiating mechanism of the boiling crisis and impacts from different variables. It can be also implemented as a sub-model in CFD codes.

Keywords: Critical heat flux (CHF), boiling heat transfer, pool boiling, forced convective boiling, cavity activation

1. Introduction

Depending on the wetted surface fraction, boiling can occur in three modes: (partial and fully developed) nucleation boiling, transition boiling and film boiling [1]. Nucleation boiling is most efficient and associated with a very large heat transfer coefficient due to two effects: frequent wetting and de-wetting of the wall by liquid and convective transfer of steam into the bulk fluid by departing bubbles. Transition boiling occurs from the critical heat flux point (CHF) where part of the surface starts to be irreversibly covered by vapor. From then on, the heat transfer coefficient begins to decrease for temperature controlled heat transfer under unstable conditions until all the heated wall is fully covered by vapor. This is then referred to as film boiling. For power controlled heating, a sudden drop of the heat transfer coefficient leads to a rapid increase of wall temperature, which potentially leads to heater meltdown. Understanding and predicting the complex phenomena involved in CHF is necessary for the efficient and safe operation of industrial heat transfer systems, like boilers, nuclear reactors, or electronics/microchips cooling systems. In the last decades, the mechanism for the transition from nucleation boiling to CHF and further to film boiling has been widely investigated. Different system variables affecting the CHF were already identified and analyzed: pressure [2-5], local liquid subcooling [2, 6, 7, 8], mass load (in subcooled flow boiling) [9-12], heated wall length, hydraulic diameter (in subcooled flow boiling) [13, 14], wettability, roughness and porosity [15, 16, 17]. Further different theoretical models to describe the CHF, such as the Hydrodynamic Instability Model [18-22], the Near-Wall Bubble Crowding Model [23, 24], the Liquid Sublayer Dryout Model [25-28], Bubble interaction theory [29] and others [35] were also developed and compared with experiments. The most widely accepted CHF model are two hydrodynamics instability model at present: the hydrodynamics instability model proposed by Zuber [21] and Liquid Sublayer Dryout model proposed by Haramura

and Katto [26]. The hypothesis of the Zuber's model is that the down flow of fresh liquid to the heat surface is prevented by the upward flow of vapor due to the Helmholtz instability. According to Haramura and Katto's model, the CHF is also a result of the Helmholtz instability, the columnar structure of vapor stems collapses with a vapor film blanketing a thin liquid film on the heater surface. These models are widely recognized and validated with experimental results. However if CHF is only due to hydrodynamics, it is difficult to explain the influence of the heating wall conditions (roughness, wettability, thickness, material and so on) on CHF. The other problem of the present CHF models is that the occurrence of the burnout is always treated as independent of the nucleate boiling process. Sadasivan et al. [30] concluded that due to CHF occurs as the upper limit of the nucleate boiling region, it is reasonable to expect that the different physical phenomena involved in the nucleate boiling region should interact such that CHF value. A realistic CHF model would be one that is a natural outcome of the description of the high heat flux nucleate boiling region. In 2009, Kolev [29] tried to build a theory to connect the nucleation boiling and CHF. He includes the effect of the shear force generated by mutual interaction of growing and departing bubbles. This shear stress shortens the bubble life cycle, reducing the bubble departure diameter which reduces the latent heat removal per bubble cycle. When this effect becomes dominant, the CHF is approached. However, the influence of the heating surface is still missing in this model except contact angle (wettability).

Today, the assessment of system designs with respect to promotion or prevention of CHF is still based on expensive experiments. Many correlations developed from such experiments have been applied in some specific 1D codes for engineering design. However, these correlations are only valid in a limited scope of applications. Computational fluid dynamics (CFD) is an attractive way to support engineering design by 3D flow simulation in the future. It would be beneficial, if occurrence of CHF could be simulated with CFD codes. However this requires a CHF model which can clearly explain the CHF initiation mechanism from nucleation boiling. Consequently, a successful CHF model should at least:

a) be able to consider both pool boiling and flow boiling;
b) be time and position dependent to explain the local wall temperature fluctuation;
c) be able to consider the effects of wall superheat and the CHF initiation mechanism;
d) cover the effects of the surface parameters;
e) be suitable to be implemented in a CFD code.

These criteria were also partly mentioned in Zhao's work [32]. In this study we analyzed the complex mechanisms of cavity activation and heat transfer in the nucleate boiling process. From this analysis, a model of priori critical heat flux (CHF-) is inferred. Further this model is developed into formulae for pool and forced convective boiling. The calculation results are compared with experimental results from different experiments for validation.

This work applies part of idea from bubble interaction theory. Instead of pure mutual effect of bubbles, we pay attention on the thermal effect during nucleation boiling on/in the wall. We also considered the mushroom structure of bubbles appear near the CHF which is well observed by experiments but with columnar of isolated bubble between the mushroom shaped bubble instead of the stem introduced by Liquid Sublayer Dryout model. Different to total sublayer dryout mechanism, we consider the columnar of bubbles dominate the CHF. This work doesn't contrary to the previous founding such as the irreversible dry spot in experiments [31, 37], because we pay attention on the priori critical heat flux where the system still have stable bubble generation when the wall temperature starts to climb. When the temperature continues climbing up to certain level like introduced ~134 °C in the experiment from Kim [31] (water horizontal pool boiling at 1 atm), the irreversible dry spot will be formed. In the other word, lower than this temperature, the wall surface still has chance to be rewetted. In this work,

we try to explain why even the rewetting does not stop the temperature climbing until irreversible dry out is formed and CHF is approached.

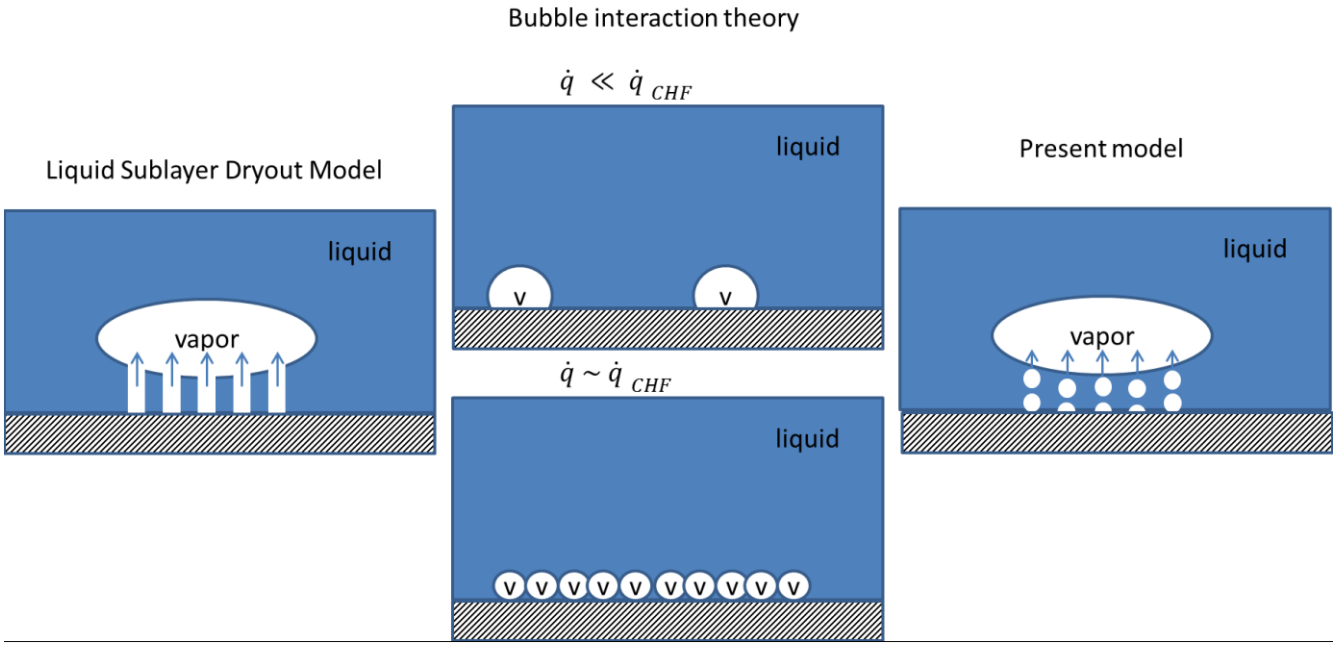

Figure 1: Typical Liquid Sublayer Dryout Model, bubbl interaction theory and new estimated bubble nucleation structure under mushroom shaped bubble

2. Results and Discussion

2.1 Concept

In this paper we fundamentally consider the bubble growth process in nucleation boiling as a stable and repeating process, which consists of cavity activation, bubble growth, bubble departure and associated surface rewetting. This concept is widely accepted and has been described in many other papers [24, 36, 48]. In the following we will derive our CHF- model by considering in detail characteristic durations, heat fluxes, and temperatures of wall, steam and bulk liquid for the different phases in nucleate boiling. While our analysis incorporates some models developed by other researchers, the key novelty of our approach is that CHF is considered as being initialized from nucleation on/in the wall and dealing with the recovery of cavity activation and thermal layer.

A commonly accepted prerequisite of nucleate boiling is the existence of nucleation sites, which are assumed to be small micrometer size cavities in the wall. It is further assumed that in the period of rewetting after a bubble departure there is always a tiny amount of vapor remaining captured in the cavities. We need to note here, that this is a model only, but one which is strongly supported by observations [33- 35]. The model assumptions for activation of a bubble are as follows.

The gas pocket in a cavity is considered as the seed for the subsequent bubble growth. It is at pressure

$$p = p_0 + p_S = p_0 + \frac{2\sigma}{r_c}. \tag{1}$$

with p_0 being the pressure in the bulk liquid, p_S the Laplace pressure of the gas-liquid interface and r_c is the critical nucleus radius for bubble grows. The heater wall is superheated at temperature $T_{wall} = T_y(0) = T_{sat}(p_0) + \Delta T_{sup}$ and has an exponential temperature profile into the bulk liquid. In

the second stage, called bubble growth, the overheated gas pocket in the cavity is further fed by evaporating liquid from the superheated liquid in the thermal boundary layer. When the bubble is still small, its growth in diameter is quite fast and determined by the inertia of the liquid being displaced. Hence this period is referred to as inertia-controlled growth. As near-wall shear stress hinders displacement of liquid in the very vicinity of the wall, a small micrometer size layer of liquid remains at the wall underneath the bubble. It is referred to as micro-layer. As superheat is highest in this layer, it subsequently contributes a lot to evaporation and disappears with time. After a while the growth of bubble diameter becomes slower and it is no longer limited by liquid displacement but by evaporative heat flux and hence heat flux through the gas-liquid interface. This period is referred to as thermal diffusion controlled growth. The third stage of the bubble cycle is bubble departure from the wall, which may be preceded a sliding motion along the wall. Immediately after bubble departure liquid from the near wall region replaces the disappearing gas volume. This is the fourth phase, or quenching phase. As the replenishing liquid is on average cooler than the unaffected liquid portions near the wall it needs to be reheated such that the thermal boundary layer over the wall is restored. All the stages have certain durations. Most important is the total growth period t_g and the waiting time t_w between bubble departure and new activation.

The above description of the bubble cycle is state of the art. In the following we will further develop this concept by bringing effects in the wall around the cavity into play. In the following we will qualitatively describe our concept and in the next sections derive equations to quantitate the effects.

Firstly we define the relevant heat fluxes. The total transferred heat Q_b during bubble growth consists of three parts: heat flowing from the wall into the bubble via evaporation $Q_{b,w}$, heat flowing from the superheated liquid near the wall into the bubble $Q_{b,s}$ and condensation heat loss at the upper part of the bubble $Q_{b,c}$, that is, heat flowing out of the bubble into the bulk liquid. The importance of this concept lies in the fact that the bubble growth is fed with heat from two sources, the wall and the thermal boundary layer, though we cannot say for the moment, how the share is quantitatively. After bubble departure, a waiting time is required to reform the nucleus in the cavity and to recover the thermal layer, that is, to recover the consumed heat in the bulk. During this period of quenching, the heat Q_q will be delivered from wall to the liquid. As during bubble growth the liquid in the vicinity of the bubble has gained the heat $Q_{b,c}$ and lost the heat $Q_{b,s}$, we may assume that $Q_q = Q_{b,s} - Q_{b,c}$. Moreover, some heat is needed to reheat the trapped liquid in the cavity from the wall. However, due to the small liquid volume in the cavity, this term can readily be neglected. The heat balance can then be written as

$$Q_{b,w} + Q_q = Q_{b,w} + Q_{b,s} - Q_{b,c} = Q_b. \tag{2}$$

Further on we define the projective area $A_b = \pi {r_d}^2$ of a fully developed bubble with departure radius r_d as the apparent heat transfer area for boiling heat transfer per single bubble. In this work, we consider that before CHF is approached, the bubble is still able to complete its departure process on the wall and accumulate near the wall to form big bubbles or mushroom structure (See *Figure 1*). Due to the waiting time is quite small for large value of superheat [42] we consider the influenced factor of bubble projective area is 1 when CHF is approached. The total transferred heat Q_b is given by $\frac{4}{3}\pi {r_d}^3 \rho_g h_{fg}$ where ρ_g is density of vapor and h_{fg} is the latent heat of the fluid. The heat flux in this area during bubble growth in the low subcooling case (*Figure 2* b) is then given as

$$\dot{q} = \frac{Q_{b,w} + Q_q}{\pi {r_d}^2 (t_g + t_w)} = \frac{Q_b}{\pi {r_d}^2 (t_g + t_w)} = \frac{(\frac{4}{3}\pi {r_d}^3 \rho_g h_{fg})}{\pi {r_d}^2 (t_g + t_w)}, \quad (3)$$

where t_g is the growth time and t_w is the waiting time.

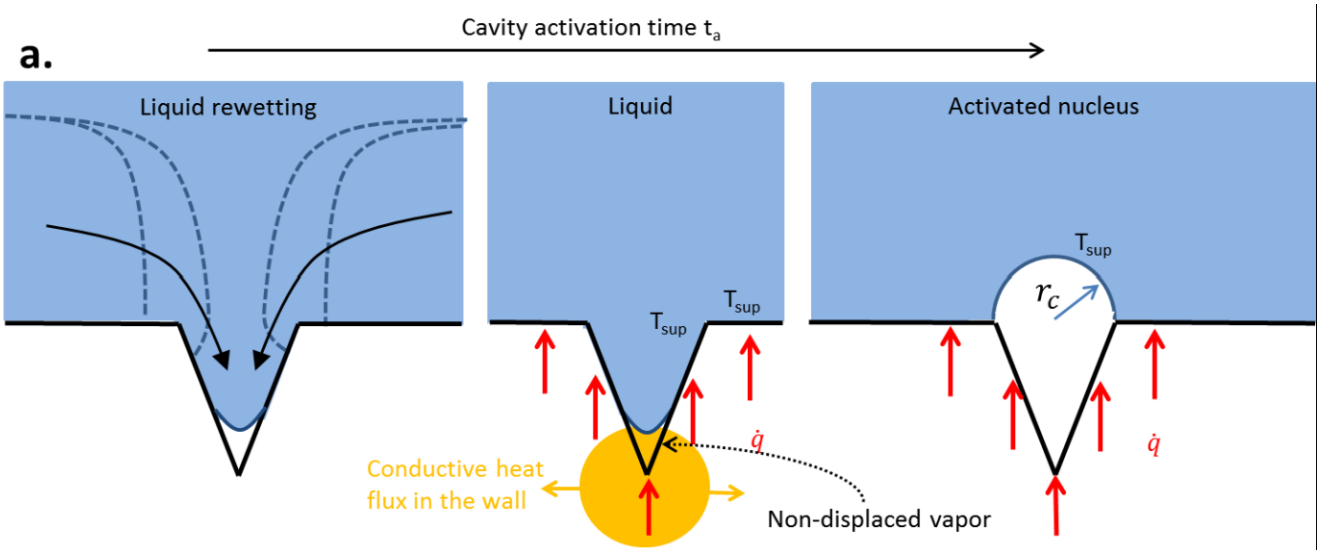

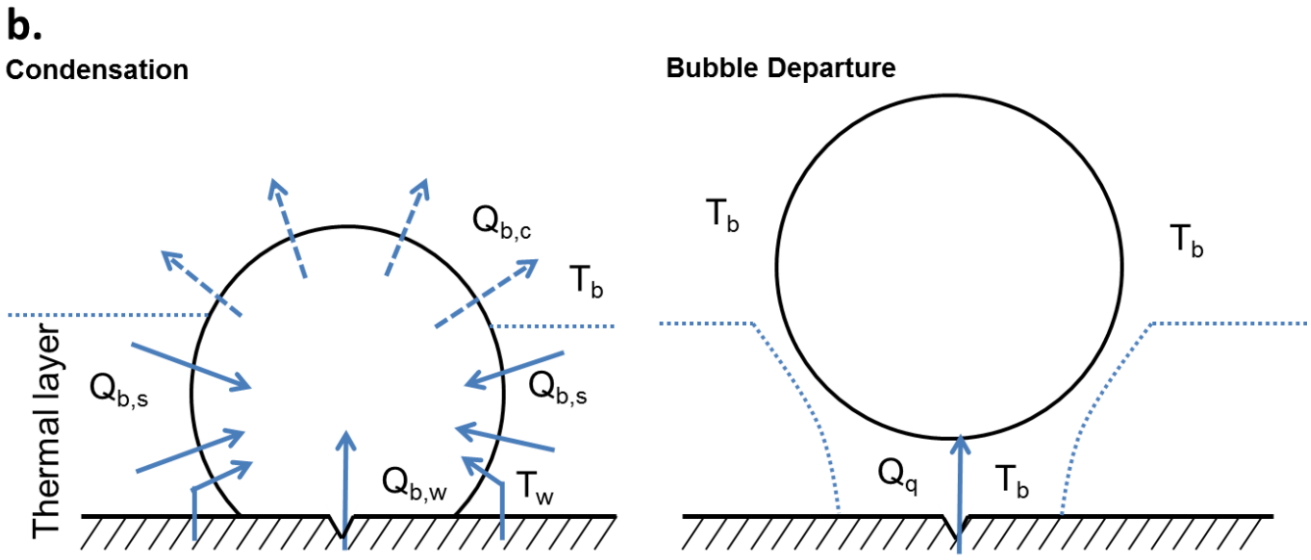

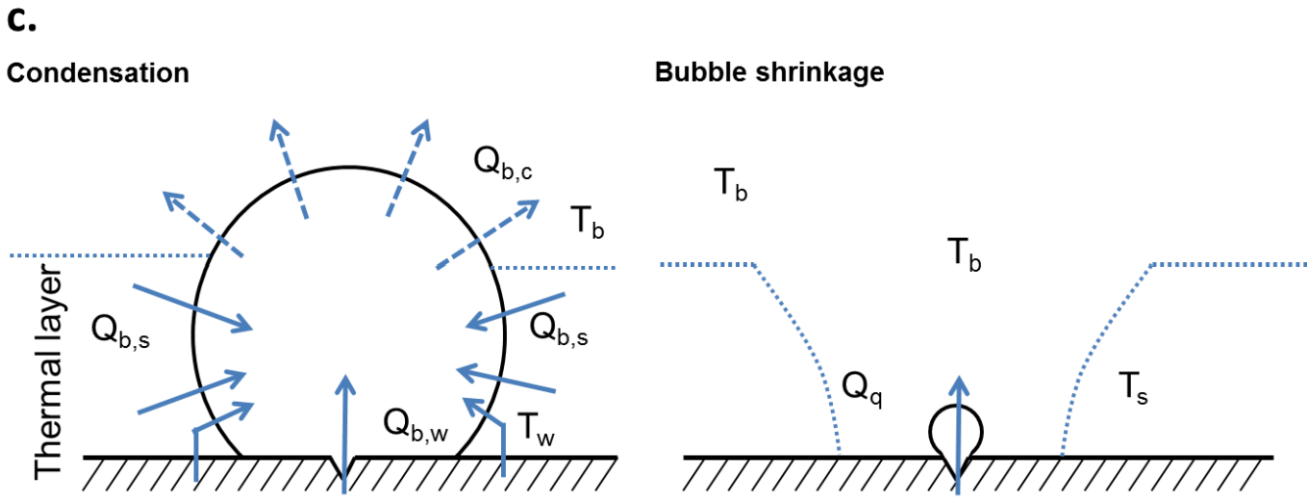

Figure 2: a) Cavity activation and heat transport during and after bubble growth: b) bubble departure in the low subcooling case and c) bubble shrinkage in the high subcooling and high heat flux case in horizontal pool boiling.

Now, to complete the picture of nucleate boiling, we will further consider the case of strong subcooling (*Figure 2* c). Then the bubble will not depart from the wall but condense when its cap penetrates into subcooled bulk liquid regions. Hence the bubble will activate, grow, shrink and collapse on the heated wall. For this case the heat flux is

$$\dot{q} = \frac{Q_b}{\pi {r_d}^2 (t_g + t_c + t_w)} = \frac{(\frac{4}{3}\pi {r_d}^3 \rho_g h_{fg})}{\pi {r_d}^2 (t_g + t_c + t_w)}, \tag{4}$$

where t_c is the condensation time. For $t_c = 0$ Equation (4) equals Equation (3). During rewetting the replenishing liquid partially displaces the vapor in the cavity [32, 34]. Before the bubble cycle closes it takes a time period t_a (cavity activation time) to form a new vapor nucleus with critical radius r_c on the mouth of cavity, which is the activation condition. The formation of this vapor nucleus requires superheating of liquid in the cavity to overcome the high pressure in the nucleus. It is worthwhile to look at this process in more detail (*Figure 2* a)). In the upper part of the cavity liquid touches the wall and we may assume that heating up this liquid has the same time scale as above the wall outside the cavity. In the lower part of the cavity there is vapor in direct contact with the cavity wall, which gives a low heat transfer coefficient. Hence we have a microscopic "film boiling" situation on the bottom of the cavity, which leads to a stronger superheat of the wall there. Conductive heat transfer towards the liquid through the wall material is then the major heat removal mechanism. The higher the heating power the higher becomes the wall superheat at the bottom of the cavity. On the other hand, as the vapor in the lower part of the cavity presents a strong heat transfer resistance, the liquid in the center of the cavity is heated slower than in single phase conditions and evaporation into the nucleus is delayed. This effect determines the activation time t_a. In our model this activation time plays a major role. As the vapor pocket delays the heating of the liquid in the cavity, we can assume that the recovery of the thermal boundary layer (recovery time t_r) occurs faster than the reactivation of the cavity, that is $t_a > t_r$. With increasing heating power or heat flux this situation can change. The wall material at the bottom of the cavity will superheat so much, that reheating of liquid in the cavity is again synchronous

with building of the thermal boundary layer outside the cavity, that is, $t_a = t_r$. If the heat flux further increases, the activation time becomes even shorter, the vapor nucleus grows rapidly into the yet not established thermal boundary layer and transfers additional heat to the boundary layer, then $t_a < t_r$. The larger one of t_r and t_a decides the total waiting time, that is, $t_w = max(t_a, t_r)$. For $t_a < t_r$ the situation is unstable, as increasing vapor content in the cavity will further increase cavity wall superheat and further shorten t_a. Eventually the temperature of the cavity wall and the vapor becomes so high, that the rewetting liquid will be directly evaporated on the wall before it flows into the cavity. Then macro film boiling on the wall sets in. As in practice the cavity geometry is generally unknown, it is highly difficult to provide a mechanistic modelling for the heat transfer processes inside the cavity. However, the decisive point is, that $t_a = t_r$ is a significant feature of critical heat flux. As we will derive below, this criterion together with heat flux balances is sufficient to determine the onset of CHF without any further modelling of in-cavity processes. As at this point the system is still marginally stable, we consider the heat flux at this very moment as priori critical heat flux **CHF-**. With Equation (4) and $t_w = t_r$ it is given as

$$\dot{q}_{CHF-} = \frac{(\frac{4}{3}\pi {r_d}^3 \rho_g h_{fg})}{\pi {r_d}^2 (t_g + t_c + t_r)}. \tag{5}$$

2.2 Application of the CHF- model

2.2.1 Model of CHF- in Pool Boiling

For pool boiling, according to Zhao [32], the wall temperature T_w surrounding the cavity, can be obtained from

$$T_w = T_b + \frac{2\dot{q}\sqrt{t\alpha_l}}{\sqrt{\pi}k_l}, \tag{6}$$

where T_b is bulk temperature, k_l is the liquid thermal conductivity, α_l is the liquid thermal diffusivity. Here, $\dot{q}$ is the feeding heat flux. For the recovery of the thermal layer, under constant heat flux, the thermal layer recovery time is derived as [32]

$$t_r = \left[\frac{\pi k_l}{2\dot{q}}\right]^2 \frac{(T_w - T_b)^2}{\pi\alpha_l}. \tag{7}$$

For a more detailed quantification of the bubble growth process we will now follow the concept of Mikic [38] developed in 1970. In this approach the bubble growth period is divided into two parts: 1) growth controlled by inertial forces and following that 2) growth controlled by the energy transfer through the vapour-liquid interface, referred to as thermal diffusion controlled period. From this assumption Mikic derived a general relation including both inertia and thermal diffusion controlled phenomena for the bubble growth rate in a dimensionless form given as

$$r^+ = \frac{2}{3}\left[(t^+ + 1)^{\frac{3}{2}} - (t^+)^{\frac{3}{2}} - 1\right] \tag{8}$$

with $r^+ = Ar/B^2$, $t^+ = A^2 t/B^2$,

$$A = \left(\frac{\pi}{7}\frac{h_{fg}\rho_g \Delta T_{sup}}{\rho_l T_{sat}}\right)^{\frac{1}{2}} \tag{9}$$

$$B = \left(\frac{12}{\pi}\alpha_l\right)^{\frac{1}{2}} Ja \tag{10}$$

and the Jakob number

$$Ja = \frac{\rho_l c_{pl} \Delta T_{sup}}{\rho_g h_{fg}}. \tag{11}$$

Here, $\Delta T_{sup} = T_w - T_{sat}$ is wall superheat, ρ_l is the liquid density, T_{sat} is the saturation temperature and $c_{p,l}$ is specific heat capacity of liquid. When t^+ is small ($t^+ \ll 1$) Equation (8) can be written as $r^+ = t^+$ or $r = At$ as a Rayleigh solution [38], which describes the growth under inertia control. For $t^+ \gg 1$, Equation (8) can be written as $r^+ = \sqrt{t^+}$ or $r = B\sqrt{t}$, which describes the growth in the thermal diffusion controlled period. As stated earlier, the bubble growth rate in the inertia controlled period is much higher than for thermal diffusion. As inertial growth is quite fast, we may omit this period in further calculations and just consider the thermal diffusion controlled growth, giving

$$t_g = \left(\frac{r_d}{B}\right)^2. \tag{12}$$

In the high subcooling case, we may assume that the condensation on the bubble also follows the rule of growth but opposite to evaporation with a factor B_c, which is defined as

$$B_c = \left(\frac{12}{\pi}\alpha_l\right)^{\frac{1}{2}} \frac{\rho_l c_{pl}(T_b - T_{sat})}{\rho_g h_{fg}}, \tag{13}$$

and

$$t_c = \left(\frac{r_d}{B_c}\right)^2 = t_g \frac{(T_w - T_{sat})^2}{(T_b - T_{sat})^2}, \tag{14}$$

The right-most term has been derived by combining Eqs. (10)-(13).
Now Equation (5) yields

$$\dot{q} = \frac{Q_b}{\pi {r_d}^2 (t_g + t_c + t_w)} = \frac{\frac{4}{3}\pi {r_d}^3 \rho_g h_{fg}}{\pi {r_d}^2 \left(t_g \left[1 + \frac{(T_w - T_{sat})^2}{(T_b - T_{sat})^2}\right] + t_w\right)}. \tag{15}$$

Note, that we have readily assumed that the gas in the bubble and the condensed liquid around it is always at saturation temperature (*Figure 2* c). Then for low subcooling we can also assume, that the same holds for the rewetting liquid, as this is a mixture of the liquid surrounding bubble.

To keep notation less complex in the following we will introduce here the latent heat $H_s = \rho_g h_{fg}$ and the parameter $X = \left(1 + \frac{(T_w - T_{sat})^2}{(T_b - T_{sat})^2}\right)$. Inserting Equation (7), Equation (12) and Equation (14) into Equation (15), we get

$$\dot{q}_{CHF-} = \frac{B^2}{2Xr_d}\left[\frac{4}{3}H_s - \sqrt{\left(\frac{4}{3}H_s\right)^2 - \frac{X\left(k_l(T_w - T_{sat})\right)^2\pi}{\alpha_l B^2}}\right]. \tag{16}$$

Equation (16) states that in horizontal pool boiling $\dot{q}_{CHF-}$ is dependent on wall superheat and bulk temperature, i.e. $\dot{q}_{CHF-}$ increases with increasing wall superheat under constant bulk temperature. The cavity with lowest activation superheat (boiling onset) has the lowest $\dot{q}_{CHF-}$ on the wall where the boiling crisis should start. In the horizontal pool boiling, the departure diameter for saturated boiling maybe calculated by the Fritz equation [39] as

$$D_{dp} = 0.0208\theta\left({}^{\sigma}/_{g(\rho_l - \rho_g)}\right)^{1/2}, \tag{17}$$

where θ is liquid-solid contact angle, g is gravitational acceleration. Cole [40] further developed this formula and Cole and Rohsenow [41] derived an expression for the departure diameter by considering only the impact of differential pressure through Ja^* as

$$D_{dp} = C\left({}^{\sigma}/_{g(\rho_l - \rho_g)}\right)^{1/2}\left({}^{\rho_f c_{pl} T_{sat}}/_{\rho_g h_{fg}}\right)^{5/4} = C\left({}^{\sigma}/_{g(\Delta\rho)}\right)^{1/2}(Ja^*)^{5/4} \tag{18}$$

with $C = 1.5 \times 10^{-4}$ and $Ja^* = {}^{\rho_l c_{pl} T_{sat}}/_{\rho_g h_{fg}}$ for water. All the equations above are for single bubbles. In reality, when the boiling process is near CHF, the bubble nucleation is considered as fully developed, which means that a large amount of bubbles will be generated from the wall and the impact from neighbouring bubbles cannot be neglected. In 1994, Kolev [42] included the bubble mutual interaction into the calculation of bubble diameter. Due to the mutual effect, the bubble will depart or lift off earlier under the action of the shear force

$$F_{d,t} = 0.3\pi\rho_l\left(2r_{d,c}\bar{\bar{V}}'\right)^2, \tag{19}$$

induced by the growth of neighbouring bubbles. Here, $\bar{\bar{V}}'$ is the time averaged fluctuation velocity or micro-convection velocity. Under large heat flux near CHF, the average fluctuation velocity was given by Kolev as

$$\bar{\bar{V}}' = B^2(\pi N)^{1/2}, \tag{20}$$

with N=$\frac{1}{\pi r_{d,c}{}^2}$ being the local nucleation site density under the mushroom shaped bubble (See *Figure 1*). Kolev already derived a solution to calculate the bubble departure diameter under different wall superheat [42]. However, we focus on the impact of the average mutual effect on the bubbles of the cavity activated at boiling onset, which this solution cannot account for. Though the inertia controlled

growth time is quite short and does not much influence the thermal transfers, it still dominates the average fluctuation velocity. With the average fluctuation velocity derived in Kolev's work, Equation (20) can be modified as

$$\bar{\bar{V}}' = 2\bar{A}^2\bar{\tau_g}(\pi N)^{1/2} = 2\bar{A}^2\bar{\tau_g}\frac{1}{r_{d,c}} \approx \bar{A} = \left(\frac{\pi}{7}\frac{h_{fg}\rho_g\overline{\Delta T_{sup}}}{\rho_l T_{sat}}\right)^{\frac{1}{2}} \propto \left(\frac{\overline{\Delta T_{sup}}}{Ja^*}\right)^{\frac{1}{2}}. \quad (21)$$

Here, $\bar{\tau_g}$ is the average bubble growth time. As the activation temperature for two neighboring cavities may be different, the averaged wall superheat $\overline{\Delta T_{sup}}$ is used here to calculate the average fluctuation velocity. We consider that the wall superheat has much less impact to the mutual effect than Ja^* or density and saturation temperature under different pressure. For example, Sugrue [55] reported under same other conditions, from 1 bar to 5 bar, the $\overline{\Delta T_{sup}}$ has nearly no considerable change while vapor density increases 5 times and saturate temperature increases 52%. As both mutual effect and departure diameter are functions of Ja^*, we estimate the bubble departure diameter near the CHF $r_{d,c}$ as

$$r_{d,c} = C^*\left({}^{\sigma}/_{g\Delta\rho}\right)^{1/2} Ja^{*n}. \quad (22)$$

When Equation (22) is inserted into Mikic's bubble growth equation under thermal diffusion control, the departure diameter is given as

$$r_{d,c} = \frac{B^2}{A}\sqrt{t_g^+} \quad (23)$$

with

$$t_g^+ = C^{*2}\theta^2\left({}^{\sigma}/_{g\Delta\rho}\right)A^2B^{-4}Ja^{*2n}. \quad (24)$$

The term $\sqrt{\left({}^{\sigma}/_{g\Delta\rho}\right)}$ in Equation (22) is commonly called the "capillary constant of liquid" [43], which can be considered as a property of the liquid. We calibrate the model and compare it with the data from Sakashita [18, 19]. We directly took the onset temperature at different pressure from the experimental data [19] as a correlation $\Delta T_{sup} = -1.94\ln(p) + 32.261$. The dependency of the liquid contact angle on the temperature is also accounted for by the expression $\theta[deg] = 157 - 0.55T[°C]$ [19]. Due to the small heater surface diameter in this particular vertical boiling experiment (7 mm) and because the experimental results are not obviously different from horizontal boiling ones, the impact of natural circulation to the rewetting can be neglected. The surface tension is considered as a linear function of temperature, which is $0.076 - {}^{0.076}/_{380[K]}T_{sup}$. It is found that n determines the slope of curve and C^* determines the $\dot{q}_{\mathrm{CHF}-}$ at 1 bar (See *Figure 3*). The average error $(abs(exp - sim)/\exp \cdot 100\%)$ between the calculated $\dot{q}_{\mathrm{CHF}-}$ and experimental value was considered. The n and C* value which leads to the lowest error will be selected.

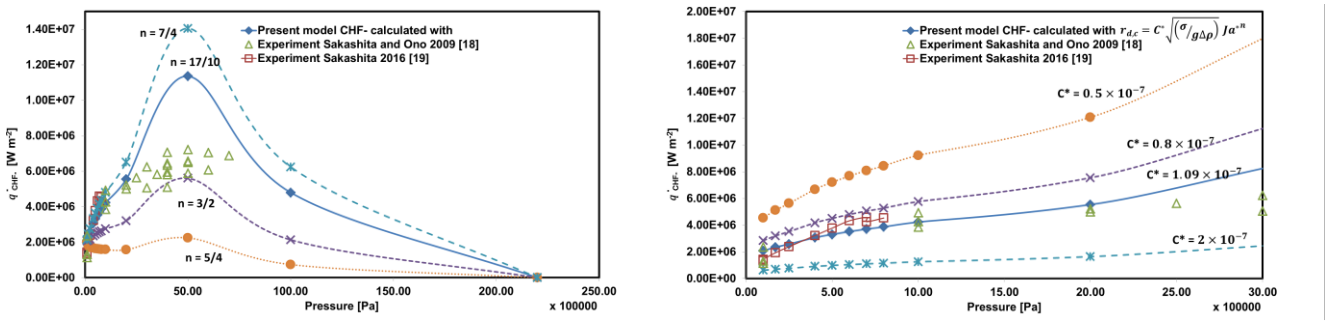

Figure 3: Predicted $\dot{q}_{CHF-}$ based on our model with "n"and "C^*" introduced in Equation (22) compared to measured CHF by Sakashita 2009 [18] and 2016 [19] for pool boiling in water at different pressures.

From the calibration we get $C^* = 1.09 \times 10^{-7}$ and $n = 1.7$ as values for water to calculate $r_{d,c}$. The bubble departure radius does also depend on the bulk temperature because the bulk temperature impacts the bubble growth and further the base diameter. So we calculate the departure radius basing on Equation (23) as

$$r_{d,c} = C_1 C^* \left(\sigma/g\Delta\rho\right)^{1/2} Ja^{*n}. \tag{25}$$

The evaporation of the superheated liquid trapped in the cavity and the microlayer on the wall (later both are called microlayer) and liquid in thermal layer surrounding the bubbles is considered as the main contribution to bubble growth. The microlayer has a superheat of $(T_w - T_{sat})$, while the thermal layer, whose temperature decreases from T_w to T_b, has an average superheat of $\left(\frac{T_w - T_{sat}}{2}\right)$ in the superheated part and subcooling of $\left(\frac{T_{sat} - T_b}{2}\right)$ in the subcooled part when the temperature profile is assumed to be linear. From the thermal diffusion controlled bubble growth rule ($r = B\sqrt{t}$), the bubble radius should be proportional to liquid superheat ΔT_{sup}. From the Kolev's work [42], it is found that the bubble departure diameter firstly increases and then decreases with increase of wall superheat. When the CHF is approached, the departure diameter decreases to a very small value. Firstly we assume the thermal layer thickness and bubble size is comparable when the process approaching CHF. Because the bubble growth time near the CHF is quite short, in saturated boiling the contribution from the superheated part of the thermal layer is simplified as $\frac{1}{2}$ of that from the microlayer due to the different superheat. However in subcooled boiling, the contribution from the superheated part of the thermal layer is only $\frac{(T_w - T_{sat})}{(T_w - T_b)}$ when the thermal layer is superheated in the saturated boiling case. Then the contribution from the superheated part of thermal layer in this case becomes $\frac{1}{2}\frac{(T_w - T_{sat})}{(T_w - T_b)}$ of that from the microlayer. The subcooling part in the thermal layer can impact bubble growth via condensation. As it was introduced in Equation (13), the condensation rate is proportional to the subcooling temperature. C_1 can then be rewritten as

$$C_1 = \frac{2}{3}\left(\frac{1}{2} \cdot \frac{(T_w - T_{sat})}{(T_w - T_b)} + 1\right) \cdot \frac{((T_w - T_{sat}))}{\left(\frac{(T_{sat} - T_b)}{2}\right)}. \tag{26}$$

This holds only when the bulk temperature $\left(\frac{T_{sat} - T_b}{2}\right)$ is larger than $(T_w - T_{sat})$. Under the same conditions, X in Equation (16) can become larger than 1. This is reasonable, but still a simplification

and future work will be directed into that direction. In this work, the molecular effusion effect [8, 11, 46] which makes the dependency of CHF on subcooling may no longer be given in the high subcooling case is not considered.

2.2.2 CHF- in forced convective boiling

We consider the flow in forced convective boiling as fully developed. The heat transfer can then be calculated with Newton's law as

$$\dot{q} = h_c(T_w - T_b). \tag{27}$$

h_c is the heat transfer coefficient and may be obtained from a Dittus-Bielter type equation [47] for multiphase fluid in a pipe as

$$h_c = 0.023\frac{k_l}{D}\left(\frac{DG(1-\varphi)}{\mu_l}\right)^{0.8}\left(\frac{\mu_l C_{p,l}}{k_l}\right)^{0.4}\cdot F \equiv \frac{\dot{q}}{(T_w - T_b)} = \frac{k_l\frac{\partial T}{\partial y}|_{y=0}}{(T_w - T_b)}. \tag{28}$$

D is the diameter of pipe, G is mass load, φ is the weight fraction of vapour and F is a function of the two-phase pressure drop which is introduced by Chen in 1966 [47].
Both of thermal diffusivity and forced convection can impact the thermal layer recovery in the forced convective boiling. From the calculation it is found that the impact of thermal diffusivity is much higher than that of convective flow. Then Equation (16) can be also applied for forced convective boiling. The departure radius is also impacted by shear stress on the wall τ_w, which is proportional to $\frac{\partial u}{\partial y}|_{y=0}$. The heat transfer coefficient h_c depends on τ_w and is a function of the mass load, the pipe diameter and length of the forced convective boiling area. The flow velocity profile is proportional to the temperature profile with function of $Pr^{1/3}$. Hence, the relationship between the heat transfer coefficient and the shear stress can be written as

$$\tau_w = \mu\frac{\partial u}{\partial y}|_{y=0} = \mu\frac{h_c u_{max}}{k_l(Pr^{1/3})^{1/7}} \tag{29}$$

with

$$u_{max} = \frac{120}{98}\bar{u} \tag{30}$$

following the turbulence 1/7 law. The surface tension force in a regular spherical bubble is given as

$$\Delta p_s = \frac{2\sigma}{r_s}. \tag{31}$$

However in the flow boiling, the bubble will be inclined as a truncated spherical bubble. But we are still able to assume the surface tension force in the wall tangential direction is C_2 times of that in the regular spherical bubble. Klausner found the ratio of surface tension force in the tangential direction to that of the perpendicular direction is around 0.4 from his experiments and concluded that compared to lift off, sliding can be easier achieved with some shear stress [48]. However, this value cannot be applied here because the bubble near CHF is far different from an ordinary bubble, that is, it has much smaller diameter and shorter growth time. Sliding happens when shear stress (τ_w) is larger or equal to

the surface tension in the tangential direction ($C_2\Delta p_s$). Hence from Equation (29) and Equation (31), we define the sliding radius as

$$r_s = \frac{C_2 \cdot 2\sigma k_l Pr^{1/21}}{\mu h_c u_{max}}. \tag{32}$$

Base on the concept introduced by Equation (3) and Equation (4), the $\dot{q}_{\mathrm{CHF}-}$ in the forced convective boiling can be written as:

$$\dot{q}_{\mathrm{CHF}-} = \frac{B^2}{2r_s}\left[\frac{4}{3}H_s - \sqrt{\left(\frac{4}{3}H_s\right)^2 - \frac{X\left(k_l(T_w - T_{sat})\right)^2\pi}{\alpha_l B^2}}\right], \tag{33}$$

Because r_s is dependent on void fraction (See Eq. (28) and (32)), the $\dot{q}_{\mathrm{CHF}-}$ in Eq. (33) is also dependent on void fraction which differs from the case of pool boiling shown in Eq. (16). However as reported by Celata and Mariani and other previous researchers [10, 49, 50], it is found that the channel orientation plays a role when the mass load is low. It means that the buoyancy impacts CHF. In our concept, it is because at low mass load, $Xr_{d,c}$ is smaller r_s and dominates the $\dot{q}_{\mathrm{CHF}-}$. If we consider this, a general formula to describe $\dot{q}_{\mathrm{CHF}-}$ can be written as

$$\dot{q}_{\mathrm{CHF}-} = \frac{B^2}{2 \cdot \min\left(Xr_{d,c}, r_s\right)}\left[\frac{4}{3}H_s - \sqrt{\left(\frac{4}{3}H_s\right)^2 - \frac{X\left(k_l(T_w - T_{sat})\right)^2\pi}{\alpha_l B^2}}\right], \tag{34}$$

This particular dependency on $Xr_{d,c}$ and r_s leads to the interpretation that CHF may occur in two different ways. One is a local phenomenon when $Xr_{d,c}$ dominates $\dot{q}_{\mathrm{CHF}-}$. The Equation (33) can be simplified as Equation (16) in this case. The CHF- will be based on local conditions and independent of the void fraction in the bulk. It usually occurs in pool boiling or forced convective boiling with low mass load. The other is a global phenomenon when r_s dominates $\dot{q}_{\mathrm{CHF}-}$. Because r_s is determined by local shear stress, the CHF- will be impacted by the void fraction in the bulk which is dependent on the conditions of upstream. It occurs in forced convective boiling with high mass load. In the global phenomenon, r_s and CHF- are strongly dependent on the global operational conditions and cannot be calculated analytically. However, it may be numerically calculated from Computational Fluid Dynamics (CFD) simulations. Hence, implementing Equation (34) into a CFD code should be a good way to calculate $\dot{q}_{\mathrm{CHF}-}$.

2.2.3 Correlations to calculate the CHF- in forced convective boiling

A correlation is required to calculate the impact of void fraction onto r_s and further $\dot{q}_{\mathrm{CHF}-}$ in Equation (34). This correlation will be recalibrated by the experimental data from Bergles [2] (See *Figure 4*). In 1963, Bergles conducted systematic experiments to study the parametric dependency of CHF for the subcooled flow boiling in circular pipes with water. In Equation (32), the departure radius r_s is a function of heat transfer coefficient h_c, which is strongly dependent on the gas void fraction. At same time the constant C_2 of the surface tension force in the perpendicular and tangential direction of the wall is also unknown. First we take one measured point as a reference point, in our case $T_{b,0} =$

19 k, $G_0 = 3038 \frac{kg}{m^2 s}$, $D_0 = 1.2\,mm$, $L_0 = 60\,mm$ and $P_0 = 207\,kPa$. Based on this reference point we get $\frac{C_2}{h_c} = \frac{0.000182}{h_{c,s}}$ with $h_{c,s}$ being the heat transfer coefficient for single phase heat transfer. Then from the available 65 data points the following correlation to calculate the term $\frac{C_2}{h_c u_{max}}$ in Equation (32) is derived

$$r_s = \frac{C_2 \cdot 2\sigma k_l Pr^{1/21}}{\mu h_c u_{max}} = \frac{0.000364 \cdot \left(\frac{D}{D_0}\right)^{0.35} \left(\frac{L}{L_0}\right)^{0.25} \left(\frac{P}{P_0}\right)^{-2.9} \left(\frac{G}{G_0}\right)^{1.15} f(\Delta T_b)}{h_{c,s} u_{max}} \cdot \frac{2\sigma k_l Pr^{1/21}}{\mu}. \quad (35)$$

Thereby $f(T_b)$ is a function of the bulk temperature T_b which is given as

$$f(T_b) = \begin{cases} \left(\frac{26\,[k]}{\Delta T_b} \cdot \frac{h_{c,s}}{h_{c,s,0}}\right)^{0.25} & \Delta T_b > \; 26\,[K] \cdot \frac{h_{c,s}}{h_{c,s,0}} = 7.32 \times 10^{-4} [K^2 m^2 W^{-1}] h_{c,s} \\ 1 & \Delta T_b \leq \; 7.32 \times 10^{-4} [K^2 m^2 W^{-1}] h_{c,s} \end{cases} \quad (36)$$

$h_{c,s,0} = 3.55 \times 10^4$ W m^{-2} K^{-1} is the single phase heat transfer coefficient at the reference point calculated with Eq. (28) with $F = 1$ and $\varphi = 0$. The calibration also based on the average error between calculated $\dot{q}_{\mathrm{CHF}-}$ and experimental error. The calibration process and the impact of different variables in Eq. (35) and C_2 are shown in *Figure 4*. CHF usually happens randomly without any schematic order at the downstream part near the end or just at the end of pipe or channel [51-54]. In our case, for simplification, we consider that CHF always happens at the end of the pipe. The excess bulk temperature measured in the Bergles' case is ΔT_b in the calculation of r_s.

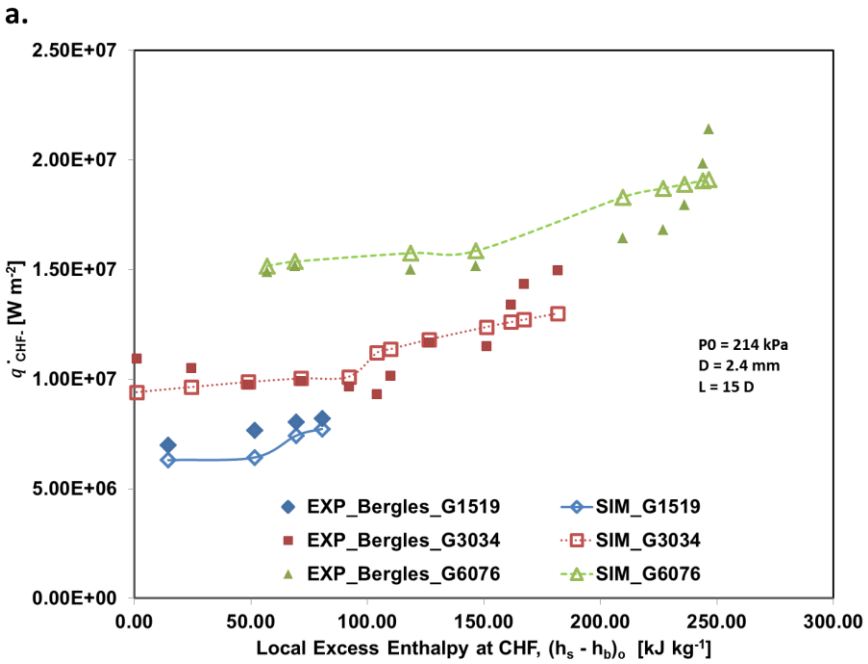

b.

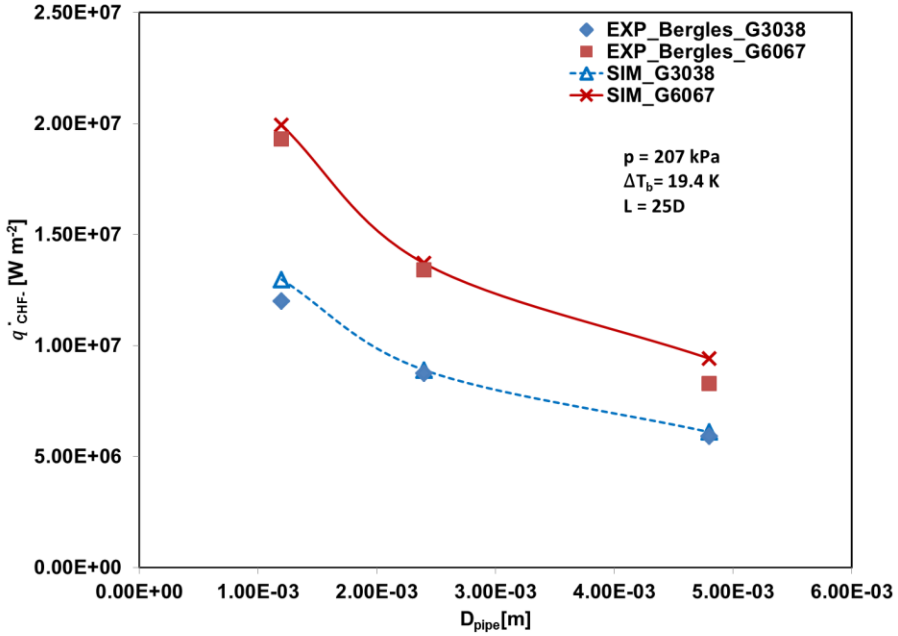
EXP_Bergles_G3038
EXP_Bergles_G6067
SIM_G3038
SIM_G6067
p = 207 kPa
ΔTb= 19.4 K
L = 25D
q'CHF- [W m-2]
Dpipe[m]
2.50E+07
2.00E+07
1.50E+07
1.00E+07
5.00E+06
0.00E+00
0.00E+00
1.00E-03
2.00E-03
3.00E-03
4.00E-03
5.00E-03
6.00E-03

419

c.

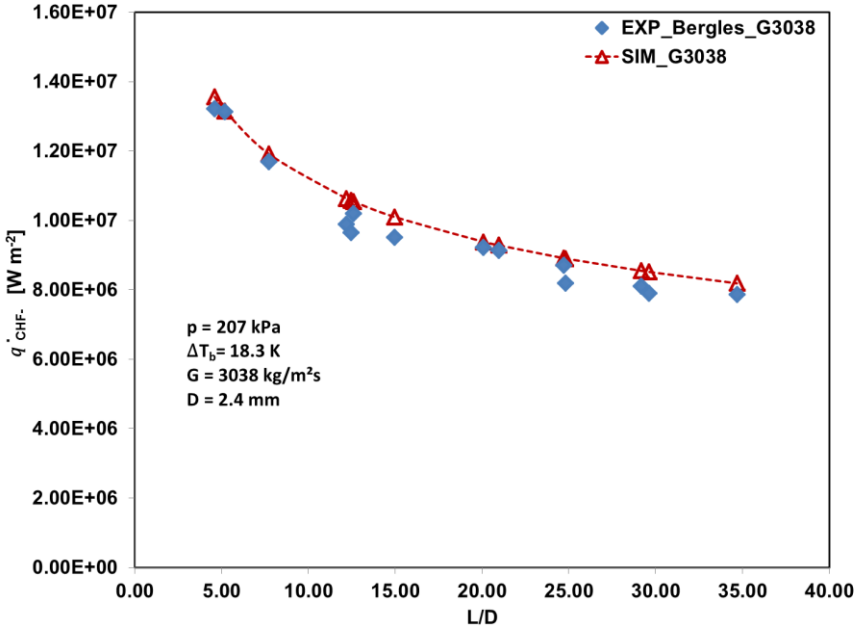
EXP_Bergles_G3038
SIM_G3038
p = 207 kPa
ΔTb= 18.3 K
G = 3038 kg/m²s
D = 2.4 mm
q'CHF- [W m-2]
L/D
1.60E+07
1.40E+07
1.20E+07
1.00E+07
8.00E+06
6.00E+06
4.00E+06
2.00E+06
0.00E+00
0.00
5.00
10.00
15.00
20.00
25.00
30.00
35.00
40.00

420

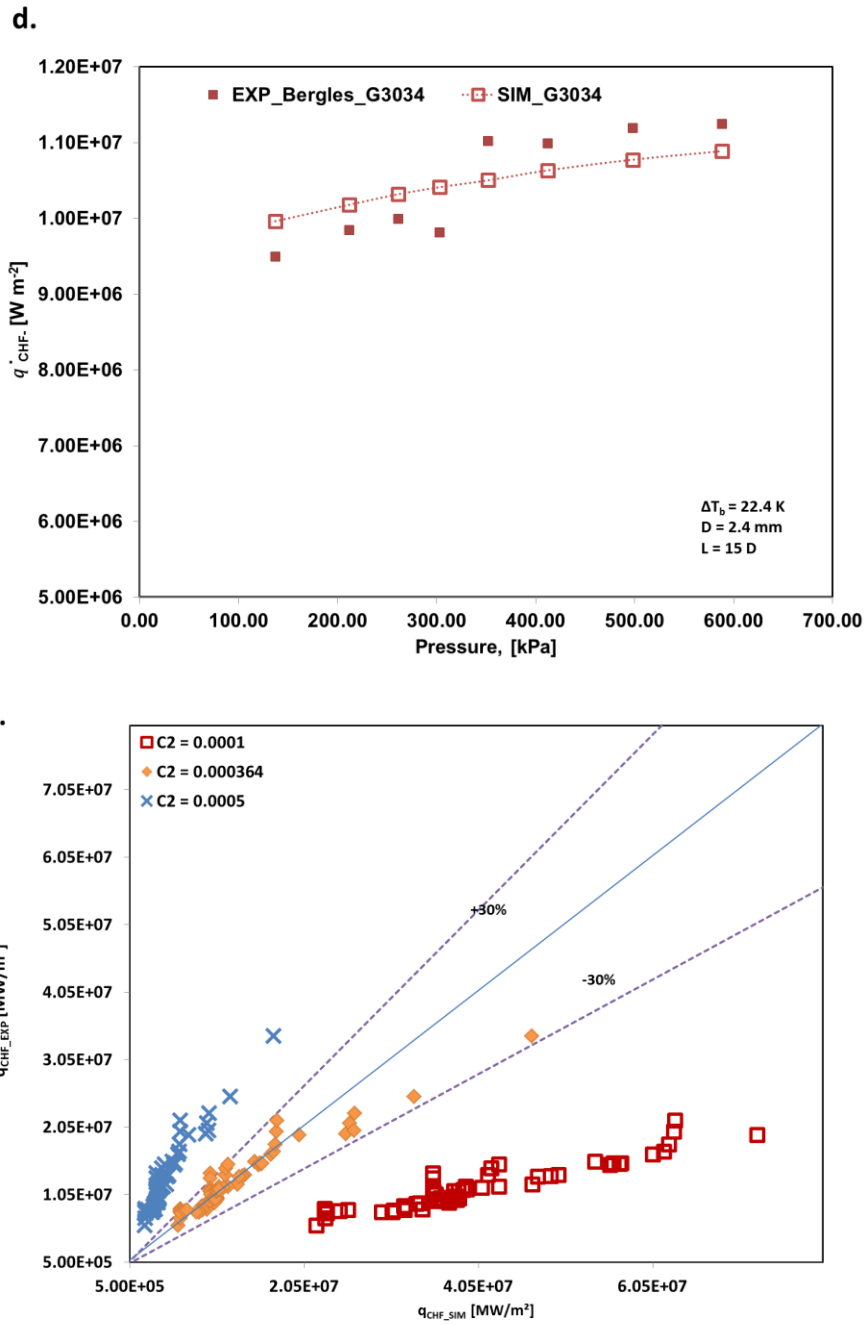

Figure 4: Modeled and experimentally measured $\dot{q}_{CHF-}$ (Bergles [2]) with a) subcooling (given as local excess enthalpy in the plot); b) different pipe diameters (D); c) length diameter ratio (L/D), d) pressure (p) and e) sensitivity analysis of constant C_2.

The average error between the correlation and the experimental data from Bergles is around 9%. This correlation is preferred to be applied to validate the CHF calculation of other forced convective boiling cases under other operational conditions. Due to the correlations are made from the experiments of circular pipe with water, the present model is only limited for the boiling process in a circular pipe with water.

At present, due to the lack of information about the boiling onset, a calibration from the experimental data is needed. This calibration even can bring the impact of the wall thickness into the $\dot{q}_{CHF-}$ calculation.

3. Validation

As is introduced, in the model there are three parameters are generated from former experiments: C^* and n are used to include the mutual effect and C_2 is used to include the bulk void fraction in the pipe. These three parameters are fixed and further applied in the validation with other experimental data.

In 2007, Gerardi [37] performed a series of saturated pool boiling experiments with de-ionised water. He employed an IR camera and a high speed camera to observe the boiling process on an ITO heater and sapphire substrate. The measured CHF is an average value from three cases. The measured onset superheat is ~ 7 K. The average liquid contact angle of de-ionised water with the heater is 90°. With that the critical departure diameter $r_{d,c}$ is calculated as 6.25×10^{-5} m. With Equation (34) we calculate the value of $\dot{q}_{\mathrm{CHF-}} = 1.06 \times 10^{6}\ \mathrm{W\ m^{-2}}$ while the averaged experimental value is 9.74×10^{5} W m^{-2}. The difference is ~ 8.8% $((EXP - CAL)/EXP \times 100\%)$.

Also we compared our model with the experiments of Tanaka et al. [7], that is horizontal pool boiling with water under 1 atm, with different subcooling temperatures (0 – 70 K) (See *Figure 5*). In this case, the onset temperature of boiling is unknown. We firstly calibrate the onset superheat based on the CHF value in the saturated boiling case and the value is found as 7.9 K. The average error is around 31% because the molecular effusion effect is not considered in this work.

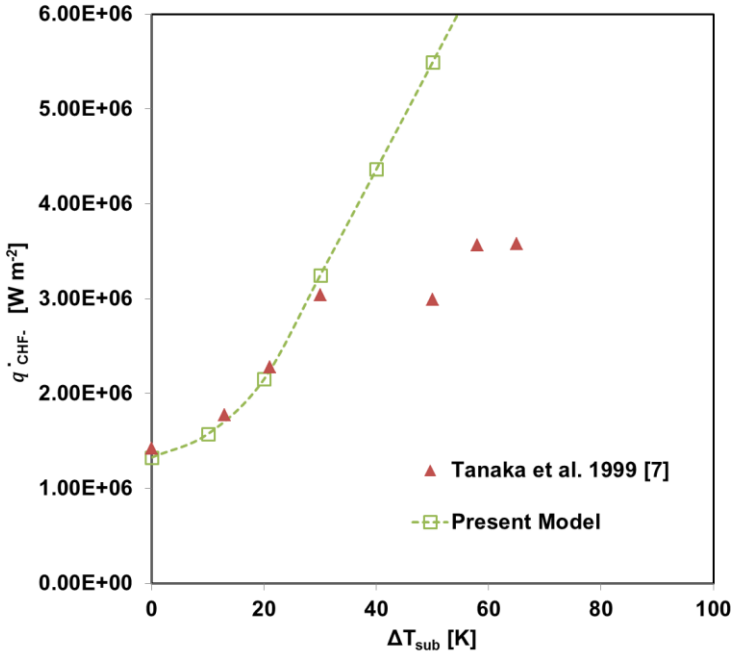

Figure 5: Measured and predicted $\dot{q}_{CHF-}$ in pool boiling as a function of subcooling when molecular effect is not considered (experimental data from Tanaka et al. [7] with water at 1 atm pressure).

In the case of Sakurai and Shiotsu [6] the authors provided a data set for horizontal pool boiling of water at one atmospheric pressure. The calibration is done for the onset wall superheat based on the case at saturated boiling. The onset wall superheat is 8.8 K. The average error for the complete calculation is ~ 6 % for both horizontal case. Different to the Tanaka's case, the molecular effusion effect doesn't present in the Sakurai and Shiotsu's case (See *Figure 6*).

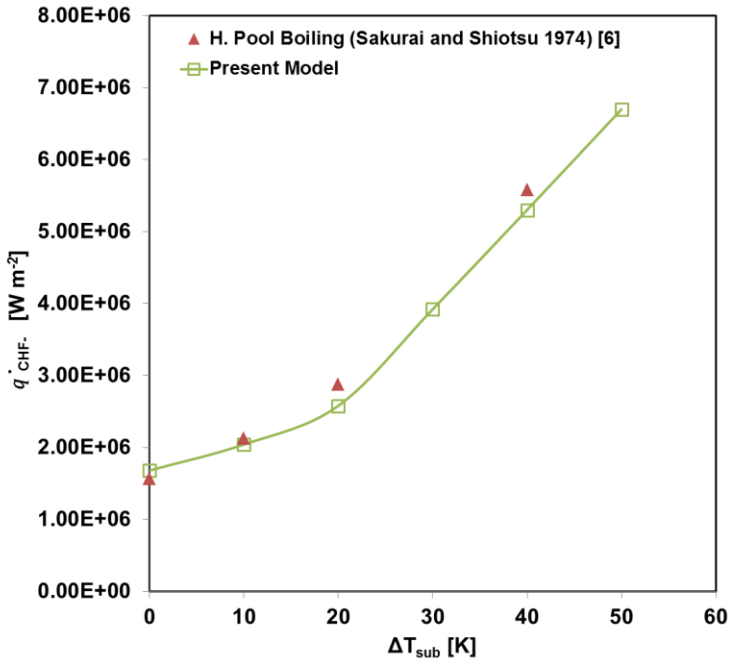

Figure 6: Measured and predicted $\dot{q}_{CHF-}$ in horizontal when molecular effect is not considered (experimental data from Sakurai and Shiotsu [6] with water at 1 atm pressure).

The CHF- model with the correlation from Bergles [2] for forced convective boiling was also validated with data from Celata [44] and Mudawar [45]. The experimental conditions are listed in the Table 1.

Table 1 Operational conditions of experiments for water.

	Gerardi	Tanaka et al.	Sakurai and Shiotsu	Bergles	Celata et al.	Mudawar and Bowers
Mass load (G) [kg m^{-2} s^{-1}]	p. boiling	Pool boiling	pool boiling	1519 ~ 24276	11390 ~ 40000	20000 ~134000
Pressure (P) [kPa]	100	100	100	137 ~ 588	584.9 ~ 2614	490 ~ 4890
Subcooling (ΔT_b) [K]	0	0 ~ 70	0 ~ 40	0 ~ 58	51 ~ 149	99 ~ 211
Diameter (D) [mm]	-	-	-	1.2 ~ 4.8	2.5	0.406 ~ 0.635
Length (L) [m]	-	-	-	0.01 ~ 0.08	0.1	0.0045 ~ 0.0108
Length/Diameter	-	-	-	4.5 ~ 35	40	7.9 ~ 26.6
Calibrated Onset Superheat [K]	No calibration 7	7.9	8.8	4.45 (2.07 bar)	0.54 (20 bar)	0.24, 0.28, 0.31 (at 31 bar)
Error	8.8%	31%.	6%.	9%	18%	12%

Totally around 200 data points from three different experiments under different operational conditions were considered (See *Figure 7*). In Mudawar's experiments, even two different wall materials and three wall thicknesses (stainless steel (SS-304) 0.406 mm and Cu-Ni 30% 0.500 mm and 0.635 mm) were involved. It was found that, the calibration of the onset point can account for the impact of the wall thickness in the calculation, which is shown in Table 1.

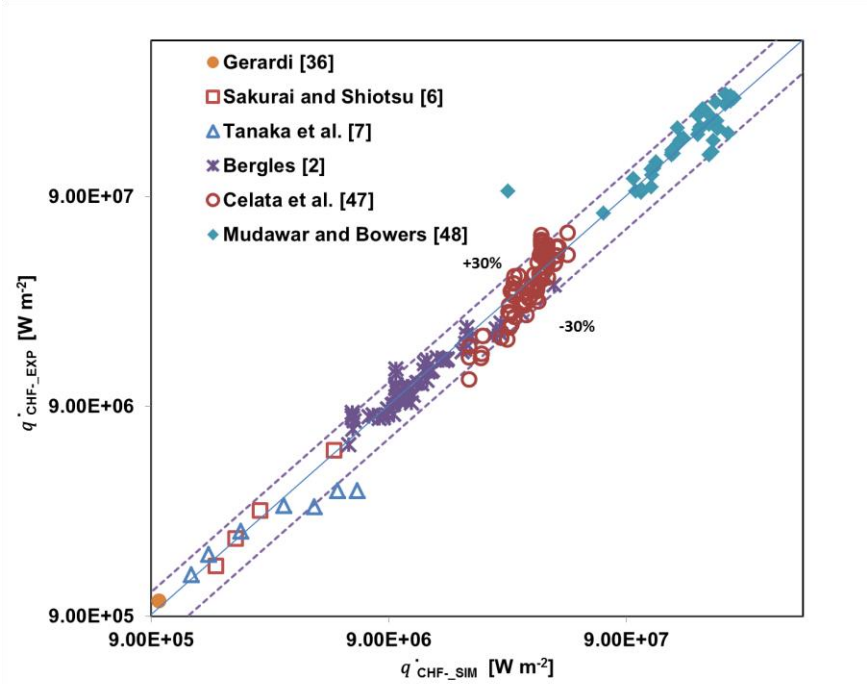

Figure 7: Measured and predicted $\dot{q}_{CHF-}$ for different experiments.

The average error for the case of Bergles is ~ 9%, but it should be noted that the correlation was derived from these data. The average error for the case of Celata is ~ 18%. The conditions of Celata and Bergles do only slightly overlap. The average error for the case of Mudawar is ~12%, which has completely different conditions compared to that of Bergles, that is, higher pressure, higher mass load, smaller diameter and shorter length. Because the present model requires the subcooled temperature at outlet as an input condition, it is still problematic for the validations with the huge amount available published CHF experimental data from literatures.

4. Conclusions and outlook

A new CHF- model and its application as a model for pool boiling and flow boiling are introduced in this paper. This model is one of the very few CHF explanations, which try to explain the boiling crisis from the view point of "on the wall" instead of "near the wall" conditions. The model accounts for the impact of the different parameters, such as pressure, orientation angle, subcooling, and mass flow, hydraulic diameter, length, pressure, orientation angle in the pool or forced convective boiling and further potentially wall thickness, wettability, surface tension and so on.

For pool boiling CHF can be considered as a local phenomenon, while for flow boiling, there are two different phenomena leading to CHF. CHF at low flow rate is similar to that in pool boiling and considered as a local phenomenon. CHF at high flow rate is found to be a global phenomenon, which strongly depends on the upstream void fraction near wall. The criterion, which one of these phenomena is relevant, is determined by the fact, which one has the main impact on the departure diameter: shear stress (hydrodynamic) or liquid property (thermal property). The CHF- model is derived from the nucleation boiling, which allows the boiling process to continuously change from nucleation boiling to CHF-. The initiating mechanism of CHF can be explained by this model. CHF will be strongly dependent on the onset wall superheat of the cavity. In the other words, the wettability and roughness can impact the onset point and impact the CHF further. Additionally the wall thickness plays a role in the heat up of the heated liquid trapped in the cavity, which can also be considered as an impacting

parameter to CHF in the future. Last but not least, our model can easily be implemented in a CFD code, which would allow modelling the whole boiling process covering the nucleation boiling and boiling crisis simultaneously in one model.

Acknowledgments

This work is funded by the German Federal Ministry of Economic Affairs and Energy (BMWi) under grant number 1501473C on the basis of a decision by the German Bundestag.

Nomenclature

A	a parameter defined as $\left(\frac{\pi}{7}\frac{h_{fg}\rho_g\Delta T_{sup}}{\rho_l T_{sat}}\right)^{\frac{1}{2}}$
$\bar{A}$	spatial average value of parameter A
B	a parameter defined as $\left(\frac{12}{\pi}\alpha_l\right)^{\frac{1}{2}} Ja$
c_{pl}	specific heat capacity of liquid
c_{pw}	specific heat capacity of wall
$C, C_{1,2} C^*$	constant or parameter
D	hydraulic diameter
F	a function of the two phase pressure drop factor
G	flow rate in a pipe
H	wall heat capacity per area
h_c	heat transfer coefficient
$h_{c,s}$	heat transfer coefficient for single liquid phase
h_{fg}	latent heat
Ja	Jakob number
Ja*	modified Jakob number $\rho_l c_{pl}\, {T_{sat}}/{\rho_g\, h_{fg}}$
k_l	liquid thermal conductivity
L	length of heated wall
N	nucleation site density
P	pressure
P_0	pressure in the bulk liquid
P_s	Laplace pressure of the gas liquid interface
Pr	Prandt number
$\dot{q}$	heat flux
$\dot{q}_{\mathrm{CHF}-}$	critical heat flux
Q	heat of bubble life cycle
Q_b	heat in the bubble
$Q_{b,c}$	heat due to condensation around the bubble
$Q_{b,s}$	heat flowing from superheated liquid surrounding the bubble
$Q_{b,w}$	heat of bubble from wall
$Q_{l,c}$	heat required to reheat the trapped liquid in the cavity
Q_q	quenching heat
Q_q	residual heat in the wall around the cavity
Q_t	latent heat of the evaporated liquid in the cavity

r	radius
r^+	dimensionless radius
r_c	critical nucleus radius
r_s	sliding radius due to shear stress
r_d	bubble departure radius
$r_{d,c}$	minimum bubble departure radius
T_b	bulk temperature
T_l	liquid temperature
T_w	wall temperature
T_{sat}	saturated temperature
T_{sub}	sub cooling temperature
ΔT_{sup}	superheat
$\overline{\Delta T_{sup}}$	average superheat of the wall
ΔT_b	subcooling
t	time
t^+	dimensionless time
t_a	cavity activation time
t_c	bubble condensation time
t_g	bubble growth time
t_r	thermal layer recovery time
t_w	bubble waiting time
τ_w	shear stress
τ_g	average bubble growth time
u_{max}	maximum velocity in the pipe
$\bar{u}$	average velocity
$\overline{\overline{V}}'$	Average fluctuation velocity
X	a parameter defined as $1 + \frac{(T_w - T_{sat})^2}{(T_b - T_{sat})^2}$
α_l	liquid thermal diffusivity
β	orientation angle
φ	weight fraction of the vapor
θ	liquid solid contact angle
σ	surface tension
μ	viscosity
ρ_g	density of vapor
ρ_l	density of liquid
ρ_w	density of wall
Δp_s	surface tension in perpendicular direction

References

[1] S. Nukiyama, “Maximum and minimum values of heat transmitted from a metal to boiling water under atmospheric pressure”, J. Soc. Mech. Eng. (Japan), vol. 37 367–374, (1934)

[2] A. Bergles, “Subcooled Burnout on Tubes of Small Diameter”, Paper No. 63 – WA – 182, ASME, (1963)

[3] A.P. Ornatskii and L.S. Vinyarskii, “Heat transfer crisis in a forced flow of underheated water in small-bore tubes”, Teplofizika Vysokikh Temperatur 3, 444-451. High Temperature 3, 400-406, (1965)

[4] C.L. Vandervort, A.E. Bergles and M.K. Jensen, “An experimental study of critical heat flux in very high heat flux subcooled boiling”, International Journal of Heat and MassTransfer 37(Suppl. 1), 161–173, (1994)

[5] G.P. Celata, “Subcooled Water Flow Boiling CHF with Very High Heat Fluxes,” Revue Generale De Thermique Fr., ISSN 0035-3159/106/9, pp. 106-114, (1992)

[6] A. Sakurai and M. Shiotsu, “Temperature-Controlled Pool-Boiling Heat Transfer,” Proceedings of the Fifth International Heat Transfer Conference, Vol. 4, B3.1, pp. 81-85, (1974)

[7] H. Tanaka, S. Nishio and R. Sugimoto, “Bubble Structure in High Heat Flux Boiling”, Proc. 36th Naitonal Heat Transfer Symposium of Japan, pp. 607 -608, (1999)

[8] W. R. Gambill, and J. H. Lienhard, “An Upper Bound for the Critical Boiling Heat FLux”, J. Heat Transfer, Vol. 111, pp. 815-818 (1989)

[9] F.C. Gunther, “Photographic Study of Surface-Boiling Heat Transfer to Water with Forced Convection,” Transactions of the ASME, Vol. 73, No. 2, pp. 115-123, (1951)

[10] G.P. Celata, and Mariani, “CHF and Post-CHF(Post-Dryout) Heat Transfer,” Chapter 17, Handbook of Phase Change, Boiling and Condensation, Edited by Kandlikar, S.G., Shoji, M., and Dhir, V.K., Taylor and Francis, New York, pp. 443-493, (1999)

[11] Shoji, M. and Zoshihara, M. Burnout Heat Flux of Water on a Thin Wire (Effect of Diameter and Subcooling). Proceedings of 28th National Heat Transfer Symposium of Japan, pp. 121-123 (1991)

[12] S.H. Chang, W.P. Baek and T.M. Bae, “A Study of Critical Heat Flux for Low Flow of Water in Vertical Round Tubes under Low Pressure,” Nuclear Engineering and Design, Vol. 132, pp. 225-237, (1991)

[13] H. Nariai, F. Inasaka, and T. Shimura, “Critical Heat Flux of Subcooled Flow Boiling in Narrow Tube,” Proceedings, ASME-JSME Thermal Engineering Joint Conference,Vol. 5, pp.455-462, (1987)

[14] H. Nariai, and F. Inasaka, “Critical Heat Flux and Flow Characteristics of Subcooled Flow Boiling with Water in Narrow Tubes,” Dynamics of Two-Phase Flows, CRC Press, pp. 689-708, (1992)

[15] S.G: Kandlikar, “Critical Heat Flux in subcooled flow boiling- an assessment of current understanding and future directions for research”, Multiphase Science and Technoliogy, Vol. 13, No. 3, pp. 207-232, (2001)

[16] V.K. Dhir, and S.P. Liaw, “Framework for a Unified Model for Nucleate and Transition Pool Boiling,” Journal of Heat Transfer, Vol. 111, pp. 3739-746, (1989)

[17] H. O'Hanley, C. Coyle, J. Buongiorno, T. Mckrell, L.W. Hu, M. Rubner and R. Cohen, "Separate Effects of Surface Roughness, Wettability and Porosity on the Boiling Critical Heat Flux", Appl. Phys. Lett. 103, no. 2: 024102, (2013)

[18] H Sakashita and A. Ono, "Boiling behaviours and critical heat flux on a horizontal plate in saturated pool boiling of water at high pressures" International Journal of heat and mass transfer, 52, 744 – 750, (2009)

[19] H Sakashita, "Critical heat flux on a vertical surface in saturated pool boiling at high pressures" Journal of Thermal Science and Technology, Vol. 11, No. 2, (2016)

[20] S.S. Kutateladze, "Heat transfer in condensation and boiling", AEC-tr-3770, pp.95-113, (1952)

[21] N. Zuber, "Hydrodynamic aspects of boiling heat transfer", AECU-4439, Physics and Mathematics, US Atomic Energy Commission, (1959).

[22] J.H. Lienhard and V.K. Dhir, "Hydrodynamic prediction of peak pool boiling". Journal of Heat Transfer, Vol.95, pp.152-158, (1973).

[23] W. Hebel, A. Detavernier, and M. Decreton, "A Contribution to the Hydrodynamics of Boiling Crisis in a Forced Flow of Water," Nuclear Engineering and Design, Vol. 64, pp. 433-445, (1981)

[24] J. Weisman, and B.S. Pei, "Prediction of Critical Heat Flux in Flow Boiling at Low Qualities," International Journal of Heat and Mass Transfer, Vol. 26, No. 10, pp. 1463-1477, (1983)

[25] Y. Katto, and Yokoya, "Proncipal Mechanism of Boiling Crisis in Pool Boiling," International Journal of Heat and Mass Transfer, Vol. 11, pp. 993-1002, (1970)

[26] Y. Haramura, and Y. Katto, "A New Hydrodynamic Model of Critical Heat Flux, Applicable Widely to Both Pool and Forced Convection Boiling on Submerged Bodies in Saturated Liquids," International Journal of Heat and Mass Transfer, Vol. 26, pp. 379-399, (1983)

[27] C. H. Lee, and I, Mudawar, "A Mechanistic Critical Heat Flux Model for Subcooled Flow Boiling Based on Local Bulk Flow Conditions," International Journal of Multiphase Flow, Vol. 14, No. 6, pp. 711-728, (1988)

[28] G.P. Celata, M. Cumo, A. Mariani, M. Simoncini, and G. Zummo, "Rationalization of Existing Mechanistic Models for the Prediction of Water Subcooled Flow Boiling Critical Heat Flux," International Journal of Heat and Mass Transfer, Vol. 37, Supplement 1, pp. 347-360, (1994)

[29] N. I. Kolev, "To the nucleate boiling theory" Nuclear Engineering and Design 239, pp. 187-192 (2009)

[30] P. Sadasivan, C unal and R. Nelson, "Perspective: Issues in CHF Modeling- The Need for New Experiments" ASME Jounal of Heat Transfer, 117 pp. 558-567 (1995)

[31] D.E. Kim, J Song and H Kim, “Simultaneous observation of dynamics and thermal evolution of irreversible dry spot at critical heat flux in pool boiling”, International Journal of Heat and Mass Transfer 99, pp 409-424 (2016)

[32] Y.H. Zhao, T. Tsuruta and T. Masuoka, “Unified theoretical prediction of fully developed nucleate boiling and critical heat flux based on a dynamic microlayer model”, International Journal of Heat and Mass Transfer 45, 3189-3197, (2002)

[33] P. Griffith, J.D. Wallis, “The role of surface conditions in nucleate boiling,” Chemical Engineering Progress Symposium Series, no. 30, vol. 56, pp. 49-63, (1960)

[34] C.H. Wang and V.K. Dhir, “Effect of Surface Wettability on Active Nucleation Site Density During Pool Boiling of Saturated Water”, J. Heat Transfer, 115, pp. 659-669, (1993)

[35] Y. Qi and J.F: Klausner, “Heterogeneous Nucleation with Artificial Cavities”, J. Heat Transfer, 127, pp. 1189-1196, (2005)

[36] X. Duan, B. Phillips, T. McKrell, and J. Buongiorno, ”Synchronized High-Speed Video, Infrared Thermometry, and Particle Image Velocimetry Data for Validation of InterfaceTracking Simulations of Nucleate Boiling Phenomena”, Experimental Heat Transfer 26, no. 23 : pp. 169-197, (2013)

[37] C. D. Gerardi, “Investigation of the pool boiling heat transfer enhancement of nano engineered fluids by means of high speed infrared thermography”, Thesis, (2009)

[38] B.B. Mikic, W.M. Rohsenow, P. Griffith, “On bubble growth rates”, International Journal of Heat and Mass Transfer 13, pp. 657–666, (1970)

[39] W. Fritz, “Berechnung des Maximalvolumens von Dampfblasen”, Phys. Z., 36 379, (1935)

[40] R. Cole, AIChE J., “Bubble frequencies and departure volumes at subatmospheric pressures”13, 779, (1967)

[41] R. Cole and W.R. Rohsenow, “Correlations of bubble departure diameters for boiling of saturated liquids”, Chem. Eng. Profr. Symp. Ser. No. 92, 65 211, (1969)

[42] N. I. Kolev, “The Influence of Mutual Bubble Interaction on the Bubble Departure Diameter, Experimental Thermal and Fluid Science” 8 pp. 167 – 74, (1994)

[43] I.L. Pioro, W. Rhosenow, S.S. Doerffer, “Nucleate pool-boiling heat transfer. I: review of parametric effects of boiling surface”, International Journal of Heat and Mass Transfer, 47, pp 5033-5044, (2004)

[44] G.P. Celata, m. Cumo and A. Mariani, “Burnout in highly subcooled water flow boiling in small diameter tubes”. International Journal of Heat and Mass Transfer 36, No. 5 pp. 1269–1285, (1993)

[45] I. Mudawar, M. B. Bowers, “Ultra-high critical heat flux (CHF) for subcooled water flow boiling—I: CHF data and parametric effects for small diameter tubes”, International Journal of Heat and Mass Transfer 42, pp. 1405–1428, (1999)

[46] Y.H. Zhao, and T. Tsuruta, 2002, “Prediction of bubble behavior insubcooling pool boiling based on microlayer model”, JSME Int. J. Vol. 45, No. 2, pp. 346-354

[47] J.C. Chen, “Correlation for boiling heat transfer to saturated fluids in convective flow”, Ind. Eng. Chem. Res. 5 pp. 322–329, (1966).

[48] J.F. Klausner, R. Mei, D.M. Bernhard, L.Z. Zheng, “Vapor bubble departure in forced convection boiling”, International Journal of Heat and Mass Transfer 36, pp. 651–662, (1993)

[49] S. Mirshak, and R.H. Towell, 1961, “Heat Transfer Burnout of a Surface Contacted by a Spacer Ribe,” USAEC Rep. DP-262, Washingon, DC.

[50] S.S. Papell, R.J. Simoneau, and D.D. Brown, 1965, “Buoyancy Effects on Critical Heat Flux of Forced Convective Boiling in Vertical Flow,” NASA TN D-3672, 17 pages.

[51] C. Haas, T. Schulenberg and T. Wetzel Critical heat flux for flow boiling of water at low pressure in vertical internally heated annuli, Int. J. Heat and Mass Transfer 60 (2013) 380-391

[52] M.S. El-Genk, S. Haynes, S. Kim, Experimental studies of critical heat flux for low flow of water in vertical annuli at near atmospheric pressure, Int. J. Heat and Mass Transfer 31 (1988) 2291–2304.

[53] J. Rogers, M. Salcudean, A. Tahir, Flow boiling critical heat fluxes for water in a vertical annulus at low pressure and velocities, in: Proceedings of the Seventh International Heat Transfer Conference, 1982, pp. 339–344.

[54] T. Schoesse, M. Aritomi, Y. Kataoka, S.-R. Lee, Y. Yoshioka, M.K. Chung, Critical heat flux in a vertical annulus under low upward flow near atmospheric pressure, J. Nucl. Sci. Technol. 34 (1997) 559–570.

[55] R.M. Sugrue, The effects of orientation angle, subcooling, heat flux, mass flux, and pressure on bubble growth and detachment in subcooled flow boiling, Master Thesis in Nuclear Science and Engineering, Massachusetts Institute of Technology, Cambridge, MA, 2012